Surface oxidation of a quasicrystalline Al–Cu–Fe alloy: No effect of surface orientation and grain boundaries on the final state

P.J. Pinhero[a)]
Iowa State University, Ames, Iowa 50011

J.W. Anderegg
Ames Laboratory, Iowa State University, Ames, Iowa 50011

D.J. Sordelet
Ames Laboratory, Department of Materials Science and Engineering, and Department of Mechanical Engineering, Iowa State University, Ames, Iowa 50011

T.A. Lograsso
Ames Laboratory and Department of Materials Science and Engineering, Iowa State University, Ames, Iowa 50011

D.W. Delaney[b)]
Iowa State University, Ames, Iowa 50011

P.A. Thiel[c)]
Ames Laboratory and Department of Chemistry, Iowa State University, Ames, Iowa 50011

We have used x-ray photoelectron spectroscopy and Auger electron spectroscopy to examine the characteristics of oxides on two types of quasicrystalline Al–Cu–Fe samples. One type was formed by consolidation of powders, resulting in multiple grains with random surface orientations. The other was a single grain, oriented to expose a fivefold surface. Both were oxidized to saturation in a variety of environments at room temperature. We measured the elemental constituents that oxidized, the extent of oxygen-induced Al segregation, and the depth of the oxide. Under the conditions of our experiments, there was little, if any, significant difference between the two types of samples. Hence, surface orientation and bulk microstructure played little or no role on the final state of the oxide under these conditions.

Surface properties of quasicrystals[1–6] are currently under active investigation, both from the point of view of basic science and from the perspective of potential applications.[7,8] In the context of basic science, it is interesting to ask whether the surface remains quasicrystalline and whether the surface morphology is intrinsically smooth or rough.[9] From the perspective of potential applications, surface properties may be important for the reportedly low friction and low adhesion characteristics.[10–22]

One broad question, which impacts both basic and applied arenas, is whether orientation and microstructure can influence surface properties. Our goal in this paper is to focus on surface oxidation under select conditions and to answer this question. We do this by comparing oxidation characteristics of two samples. The first is a single-grain sample, oriented to expose a fivefold surface—chosen because the fivefold surfaces of icosahedral quasicrystals are generally the most stable, hence the most abundant in nature. The second sample is a monolith formed by consolidation of a fine powder. Within the latter sample, many grains are exposed at the surface, with random orientation; furthermore, there are many boundaries between the grains. Hence, this comparison should reveal the role (if any) of surface orientation and bulk microstructure in surface oxidation.

Specifically, we focus on the icosahedral (i) quasicrystal Al–Cu–Fe. We use two experimental techniques in ultrahigh vacuum. The primary technique is x-ray photoelectron spectroscopy (XPS), and the secondary technique is x-ray-induced Auger electron spectroscopy (XAES). We determine which elements in the alloy oxidize, how oxidation changes surface stoichiometry, and the average depth of the oxide layer. The samples are oxidized at room temperature in three different environments, which present increasing levels of water (humidity). This range of samples, techniques, and conditions

defines the extent to which the broad issue of surface quasicrystallography is addressed here.

Previous work has shown that i-Al–Pd–Mn and i-Al–Cu–Fe tend to form a passivating layer of pure, or nearly pure, aluminium oxide.[23–32] The oxide depth is about the same as that formed on pure Al. Previous work has also shown that increasing humidity[31,33] and increasing pressure[24] present increasingly aggressive oxidizing environments, resulting in more elements oxidized, more extensive Al segregation, and/or thicker oxide layers. These trends are also reproduced in the present work.

Experimental conditions are described elsewhere.[28,31,33,34] In brief, the single-grain sample is prepared by cyclic heat treatment.[34–36] The multiple-grain sample is prepared by hot isostatically pressing (HIPing) spherical gas atomized powders having a nominal size range between 25 and 45 microns in diameter. Note, the as-atomized powders contain grains which are in the typical range of 1–5 microns; moreover, this grain size is retained in the fully dense HIPed samples.[33] There is no detectable porosity in the HIPed monoliths. The grain size is to be compared with an analysis area of about 2 mm^2 in XPS and XAES. Hence, the XPS and XAES analyses average over millions of grains, with random orientations, in this sample. The preexisting powders are marked by oxygen-rich boundaries. However, this oxygen can be depleted from the surface and near-surface regions by sputtering and annealing to the point that no oxygen is detectable in XPS or XAES. (See top row, Fig. 1) The compositions, determined from inductively coupled plasma atomic emission spectroscopy (ICP-AES),

are $Al_{63.4\pm0.4}Cu_{24.0\pm0.9}Fe_{12.6\pm0.5}$, and $Al_{65.7}Cu_{22.2}Fe_{12.1}$ for the single-grain and HIPed samples, respectively. Powder x-ray diffraction is consistent with expectation for bulk quasicrystallinity in both types of samples.[33,35] Both samples are polished, and then sputter-annealed in ultrahigh vacuum ($P \leq 4 \times 10^{-10}$ torr), prior to oxidation.[33,34] For comparison, some data are acquired on an Al(111) single crystal, which is also sputter-annealed.

Three oxidizing environments are used: vacuum, "normal" air, and liquid water.[31,33] In vacuum, the oxidant is 99.99% pure oxygen gas. Because the oxygen is supplied through a directional doser, oxygen pressure at the sample is not known but must be greater than about 3×10^{-8} torr and is probably lower than 10^{-6} torr. The intermediate environment is "normal" air. This is a sample box in atmosphere with $CaSO_4$ desiccant. The water-rich environment is liquid water. To be placed in liquid water, the sample is removed from the UHV chamber under N_2 and immersed in micropore-purified H_2O. Each of the three types of oxidized surfaces is passivated; i.e. it does not react further in its specific oxidizing environment, as far as XPS and XAES can tell.

Elsewhere, we have presented data for the pure elements and determined the key signatures of oxidation under our experimental conditions. As a baseline, the peak positions of the pure, elemental metals, indicated by vertical dashed lines in Fig. 1, are 117.9 eV for the Al 2s line in XPS, 707.0 eV for the Fe 2p line in XPS, and 918.1 eV for the Cu $L_3M_{4,5}M_{4,5}$ transition in XAES. (Note that peak positions are given as binding energies for the XPS lines and as kinetic energies for the XAES lines.) The signatures of oxidation under our conditions
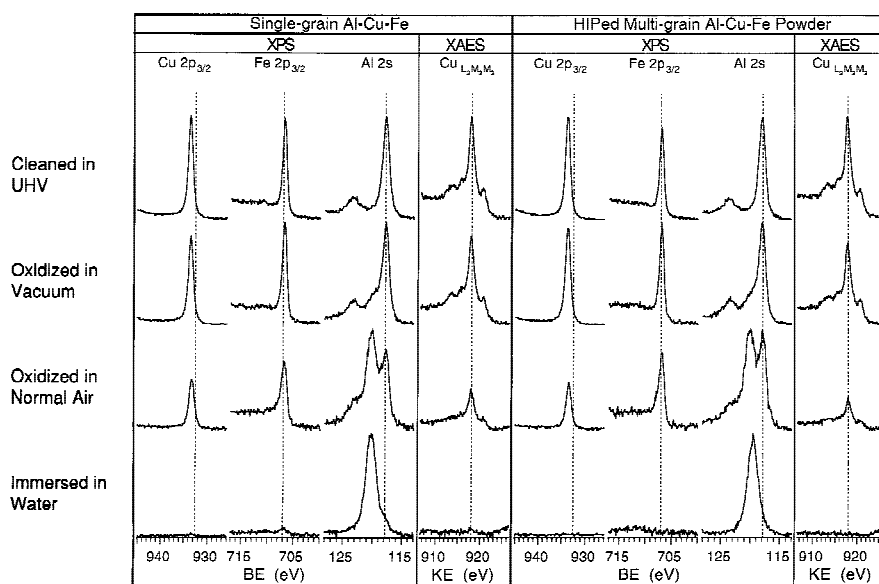

FIG. 1. XPS and XAES spectra of Al, Cu, and Fe after various treatments, at an emission angle of 45°. Within each column, the vertical dashed line shows the average peak position for the clean surface of the pure metal constituent, measured in our laboratory. Spectra are not smoothed. A horizontal background is subtracted from each XPS curve, and the curve is then normalized to the peak height of the clean surface. For instance, the Cu 2p peaks are all scaled to the top one. The Auger data are shown in the N(E) mode. Note that peak positions are given as binding energies for the XPS lines and as kinetic energies for the XAES lines.

are the development of a new peak at 120.5–121.0 eV for the Al 2s line in XPS, a new peak at 710–712 eV for the Fe 2p line in XPS, and the development of a new peak at 916.0 eV for the Cu $L_3M_{4,5}M_{4,5}$ transition in XAES. (The Cu $2p_{3/2}$ line is also shown in Fig. 1, although it is not sensitive to oxidation in these experiments.[33]) Elsewhere, we have shown that the minor components, Cu and Fe, are more likely to oxidize in the form of pure elements than as components of the alloy.[31,33] Presumably, they are protected in the alloy by preferential oxidation of Al, an effect that is observed also in some other Al-containing alloys.[37–39]

Figure 1 illustrates which components of the alloy oxidize. The top rows of Fig. 1 show the XPS and relevant XAES data for the clean single-grain and multigrain samples, respectively. Going down a single column in Fig. 1 represents a progression from a clean surface in vacuum, to a surface, which has been oxidized in vacuum, to normal air, to liquid water. This progression causes increasing attenuation of the Fe and Cu signals, relative to the Al. This attenuation can hamper the ability to detect oxidation of Fe and Cu.

The results in Fig. 1 are very similar for the two quasicrystalline samples. For both, Al oxidizes under all conditions studied here. Copper is protected from oxidation by the passivating layer, and Fe is protected also except possibly in liquid water.

It is known that oxidation causes surface segregation of Al,[23–32] changing the composition measured with XPS or XAES. Such compositions are depth-weighted averages over the top ~100 Å of material. The results are shown in Table I. For both samples, oxidation causes the expected enrichment in Al, with depletion of Cu and Fe. These effects become more marked as the oxidizing environment becomes more severe. After the harshest treatment, water immersion, the surface concentration of Al

exceeds 96% and the concentration of the other metals falls below 3%.

There has been some question about whether vacuum oxidation at room temperature can cause segregation of Al.[24] Table I shows that this effect occurs unambiguously for the single-grain sample. The change in Al concentration, in going from the clean surface to the vacuum-oxidized surface, is statistically significant (with 95% confidence) for the single-grain sample (61 → 67% Al) but not for the multigrain sample (65 → 70% Al). This is true even though the magnitude of the change in the average values is about the same (6 versus 5 at.%), because the confidence limits are narrower for the single-grain sample. This disagrees with earlier results where no surface segregation of Al was reported after vacuum oxidation at room temperature.[23,24] Pressure plays a role in determining the conditions under which an aluminium oxide film can form[24] and may account for some of the discrepancy with previous results.

The final quantity for comparison is the oxide depth, which we determine in two ways. The first is the fixed-angle method of Strohmeier,[40] and the second is the variable-angle method.[41] Details are given elsewhere.[28,31,33] The two approaches are semiindependent, although both rest upon calculation of the inelastic mean free path of the Al 2s photoelectrons in the oxide.[33]

The results are shown in Table II. Comparing values in the left and right columns serves to compare results from the two XPS techniques. It can be seen that there is agreement, with 95% confidence, in all cases. This serves as some validation of the techniques. Comparing single- and multigrain values for given conditions (i.e., making comparisons within columns) should reveal whether the microstructure of the sample plays a major role in this aspect of oxidation. This comparison shows that depths are the same after vacuum oxidation, perhaps 20% thicker on the single grain after air oxidation and perhaps 20–30% thinner on the single grain after liquid immersion. These values could also be affected if the roughness

TABLE I. Surface and bulk compositions, measured by XPS and ICP-AES, respectively. The number of measurements is given by n. The starting point for each surface measurement is a clean, sputter-annealed surface, which is then treated as indicated. Statistical uncertainties are 95% confidence limits.

Environment/sample	n	% Al	% Cu	% Fe
Bulk (from ICP-AES)				
Single grain	4	63.4 ± 0.4	24.0 ± 0.9	12.6 ± 0.5
Multigrain	1	65.7	22.2	12.1
Surface, clean in vacuum				
Single grain	13	61 ± 2.3	26 ± 1.2	13 ± 2.6
Multigrain	8	65 ± 1.8	26 ± 3.0	9.2 ± 2.0
Surface, oxidized in vacuum				
Single grain	3	67 ± 2.0	22 ± 1.1	11 ± 2.0
Multigrain	3	70 ± 3.0	22 ± 2.3	7.7 ± 1.1
Surface, oxidized in normal air				
Single grain	3	83 ± 1.1	8.3 ± 1.1	8.3 ± 2.3
Multigrain	3	88 ± 1.1	7.3 ± 1.1	5.0 ± 0.0
Surface, oxidized in water				
Single grain	6	97 ± 1.0	1.5 ± 1.1	1.2 ± 0.8
Multigrain	2	99 ± 1.4	0 ± 0	1.0 ± 1.4

TABLE II. Oxide thicknesses on the quasicrystals. The number of measurements is given by n. The starting point for each surface measurement is a clean, sputter-annealed surface, which is then oxidized at room temperature. Statistical precisions are calculated as 95% confidence limits.

Environment and phase	n	Variable angle method: oxide thickness (Å)	n	Fixed angle method: Oxide thickness (Å)
1. Vacuum O_2				
Single grain	3	4.6 ± 0.9	3	5.4 ± 1.0
Multigrain	3	5.5 ± 0.5	3	4.7 ± 1.0
Al(111)	1	5.6	1	5.2
2. Normal air				
Single grain	3	25 ± 6.5	3	27 ± 3.0
Multigrain	3	19 ± 4.1	3	21 ± 0.5
3. Liquid water				
Single grain	3	61 ± 6.9	6	67 ± 5.6
Multigrain	2	86 ± 9.6	2	86 ± 4.3

is significantly different on the two types of samples. Thus, the depth and/or roughness of the oxide may depend to a small extent upon whether the surface is single- or multigrain. The differences after air and water treatments are not entirely convincing, however, because they are not systematic.

For reference, some data for Al(111) are also shown in Table II. The oxide which forms on this single crystal is about the same depth as that which forms on both of the alloy samples, in vacuum. This is in agreement with our earlier conclusions that the oxidation chemistry of the quasicrystalline alloys at room temperature is dominated by the chemical composition (the Al content) and not the atomic structure.[33]

In summary, the oxidation chemistry is very similar for two different types of samples: a single grain of this icosahedral alloy, oriented to expose a fivefold surface, and a multigrain sample, consisting of consolidated particles. This suggests that surface orientation is not a key issue in the oxidation of these samples. It also suggests that the microstructure of the bulk sample—the density of interfaces between grains—does not play a major role in these oxidation characteristics. The broader suggestion is that studies of one type of surface can be taken as a reasonable indication of the behavior of the other type of surface.

These generalizations are limited, of course, to this specific experimental design, in particular to the icosahedral Al–Cu–Fe alloy, to the conditions of oxidation explored, and to the technique used primarily to characterize the oxides (XPS). It is possible that differences could be discovered if different techniques were used, if oxidation were carried out at elevated temperatures, or if kinetics were measured rather than final states.

ACKNOWLEDGMENT

REFERENCES

1. D. Shechtman, I. Blech, D. Gratias, and J.W. Cahn, Phys. Rev. Lett. **53,** 1951 (1984).
2. D. Shechtman and I. Blech, Metall. Trans. A **16,** 1005 (1985).
3. P.W. Stephens and A.I. Goldman, Sci. Am. **264,** 24–31 (1991).
4. A.I. Goldman and M. Widom, Annu. Rev. Phys. Chem. **42,** 685–729 (1991).
5. A.I. Goldman and K.F. Kelton, Rev. Modern Phys. **65,** 213–230 (1993).
6. C. Janot, *Quasicrystals: A Primer,* Monographs on the Physics and Chemistry of Materials Vol. 48, edited by P.B. Hirsch, N. F. Mott, and R.J. Brook (Clarendon Press, Oxford, U.K., 1992).
7. D.J. Sordelet and J.M. Dubois, MRS Bull. **22**(11), 34 (1997).
8. J.M. Dubois, in *An Introduction to Structure, Physical Properties and Application of Quasicrystalline Alloys,* edited by J-B. Suck, M. Schreiber, and P. Hausler (Springer Verlag, Berlin, 1998).
9. C.J. Jenks and P.A. Thiel, MRS Bull. **22**(11), 55 (1997).
10. C. Berger, E. Belin, and D. Mayou, Ann. Chim. Fr. Mater. **18,** 485 (1993).
11. S. Takeuchi, H. Akiyama, N. Naito, T. Shibuya, T. Hashimoto, and K. Edagawa, J. Non-Cryst. Solids **153–4,** 353 (1993).
12. J.M. Dubois and P. Weinland, European Patent No. EP 0356287 and U.S. Patent No. 5 204 191 (20 April 1993).
13. J.M. Dubois, Phys. Scr. **T49A,** 17 (1993).
14. J.M. Dubois, S.S. Kang, and Y. Massiani, J. Non-Cryst. Solids **153–4,** 443–445 (1993).
15. S.S. Kang, J.M. Dubois, and J. von Stebut, J. Mater. Res. **8,** 2471 (1993).
16. J.M. Dubois, A. Proner, B. Bucaille, P. Cathonnet, C. Dong, V. Richard, A. Pianelli, Y. Massiani, S. Ait-Yaazza, and E. Belin-Ferré, Ann. Chim. Fr. **19,** 3–25 (1994).
17. J.M. Dubois, S. S. Kang, and A. Perrot, Mater. Sci. Eng. **A179/A180,** 122–126 (1994).
18. A.M. Viano, R.M. Stroud, P.C. Gibbons, A.F. McDowell, M.S. Conradi, and K.F. Kelton, Phys. Rev. B **51,** 12026–12029 (1995).
19. R.M. Stroud, S.T. Misture, A.M. Viano, P.C. Gibbons, and K.F. Kelton, Appl. Phys. Lett. **69,** 2998–3000 (1996).
20. J.M. Dubois, in *New Horizons in Quasicrystals: Research and Applications,* edited by A.I. Goldman, D.J. Sordelet, P.A. Thiel, and J.M. Dubois (World Scientific, Singapore, 1997), pp. 208–215.
21. M.F. Kelton and P.C. Gibbons, MRS Bull. **22**(11), 69 (1997).
22. J.Y. Kim, P.C. Gibbons, and K.F. Kelton, J. Alloys Compd. **266,** 311–317 (1998).
23. D. Rouxel, M. Gavatz, P. Pigeat, B. Weber, and P. Plaindoux, in *New Horizons in Quasicrystals: Research and Applications,* edited by A.I. Goldman, D.J. Sordelet, P.A. Thiel, and J.M. Dubois (World Scientific, Singapore, 1997), pp. 173–180.
24. M. Gavatz, D. Rouxel, D. Claudel, P. Pigeat, B. Weber, and J.M. Dubois, in *Proceedings of the 6th International Conference on Quasicrystals (ICQ6),* edited by S. Takeuchi and T. Fujiwara (World Scientific, Singapore, 1998), pp. 765–768.
25. C.J. Jenks, P.J. Pinhero, S-L. Chang, J.W. Anderegg, M.F. Besser, D.J. Sordelet, and P.A. Thiel, in *New Horizons in Quasicrystals: Research and Applications,* edited by A.I. Goldman, D.J. Sordelet, P.A. Thiel, and J. M. Dubois (World Scientific, Singapore, 1997), pp. 157–164.
26. S-L. Chang, C-M. Zhang, C.J. Jenks, J.W. Anderegg, and P.A. Thiel, in *Proceedings of the 5th International Conference on Quasicrystals (ICQ5),* edited by C. Janot and R. Mosseri (World Scientific, Singapore, 1995), pp. 786–789.
27. S-L. Chang, W.B. Chin, C-M. Zhang, C.J. Jenks, and P.A. Thiel, Surf. Sci. **337,** 135–146 (1995).
28. S-L. Chang, J.W. Anderegg, and P.A. Thiel, J. Non-Cryst. Solids **195,** 95–101 (1996).
29. S. Suzuki, Y. Waseda, N. Tamura, and K. Urban, Scripta Mater. **35,** 891–895 (1996).
30. T. Gu, A.I. Goldman, P. Pinhero, and D. Delaney, in *New Horizons in Quasicrystals: Research and Application,* edited by A.I. Goldman, D.J. Sordelet, P.A. Thiel, and J.M. Dubois (World Scientific, Singapore, 1997), pp. 165–168.
31. P.J. Pinhero, S-L. Chang, J.W. Anderegg, and P.A. Thiel, Philos. Mag. B **75,** 271–281 (1997).
32. C.J. Jenks, P.J. Pinhero, T.E. Bloomer, S-L. Chang, J.W. Anderegg, and P.A. Thiel, in *Proceedings of the 6th International Conference on Quasicrystals (ICQ6),* edited by S. Takeuchi and T. Fujiwara (World Scientific, Singapore, 1998), pp. 761.
33. P.J. Pinhero, J.W. Anderegg, D.J. Sordelet, M.F. Besser, and P.A. Thiel, Philos. Mag. B **79,** 91–110 (1999).
34. Z. Shen, P.J. Pinhero, T.A. Lograsso, D.W. Delaney, C.J. Jenks, and P.A. Thiel, Surf. Sci. **385,** L923–L929 (1997).
35. T.A. Lograsso and D.W. Delaney, J. Mater. Res. **11,** 2125 (1996).
36. T.A. Lograsso and D.W. Delaney, in *Proceedings of the 6th International Conference on Quasicrystals (ICQ6),* edited by S. Takeuchi and T. Fujiwara (World Scientific, Singapore, 1998), pp. 325–328.
37. A. Hoffman, T. Maniv, and M. Folman, Surf. Sci. **193,** 57–80 (1988).
38. A. Mesarwi and A. Ignatiev, J. Appl. Phys. **71,** 1943 (1992).
39. J. Libuda, F. Winkelmann, M. Bäumer, H-J. Freund, T. Bertrams, H. Neddermeyer, and K. Müller, Surf. Sci. **318,** 61 (1994).
40. B.R. Strohmeier, Surf. Interface Anal. **15,** 51 (1990).
41. C.S. Fadley, *Basic Concepts of X-ray Photoelectron Spectroscopy,* Electron Spectroscopy: Theory, Techniques, and Applications Vol. 2, edited by C.R. Brundle and A.D. Baker (Academic Press, New York, 1978).